land

MDPI

Article

Scrutinizing the Hydrological Responses of Chennai, India Using Coupled SWAT-FEM Model under Land Use Land Cover and Climate Change Scenarios

Pooja Preetha [1,*] and Mahbub Hasan [2]

[1] Department of Civil Engineering, Alabama A&M University, Huntsville, AL 35811-7500, USA
[2] Department of Civil & Mechanical Engineering and Construction Management, Alabama A&M University, Huntsville, AL 35811-7500, USA; mahbub.hasan@aamu.edu
* Correspondence: pooja.preetha@aamu.edu; Tel.: +1-256-372-4148

Abstract: This study implemented a coupled SWAT-FEM simulation model to evaluate the impacts of land use land cover and climate change scenarios (LCS) on the water resources of river catchments in Chennai, India. The land use land cover data were obtained by merging the source data from National Remote Sensing Centre (NRSC) and International Water Management Institute (IWMI). Climate change simulations were obtained from four global climate models (GCM), including GFDL Baseline Scenario (1981–2000), GFDL A1B Scenario (2081–2100), CCSM4 Baseline Scenario (1986–2005), and CCSM4 A1B Scenario (2081–2100). The LCS predicted temperature increases of 2.32 °C and 1.74 °C for GFDL and CCSM4, respectively, by the end of the century. The water use predictions suggested increases above 20% in the utilization of water by 2100, inferring the noticeable dynamics of inter-annual as well as inter-month variability in water resources in the river basins of Chennai soon. The study is novel through its implementation of a coupled modeling approach to improve the practicality of the SWAT-FEM model and to deliver useful projections of land and climate change impacts on hydrological responses. The results provide useful insights into how the variability in climate conditions alters the spatiotemporal water responses in catchment scales.

Keywords: Chennai River catchment; SWAT-FEM; land use land cover; climate change; stream flow; groundwater storage; water use

Citation: Preetha, P.; Hasan, M. Scrutinizing the Hydrological Responses of Chennai, India Using Coupled SWAT-FEM Model under Land Use Land Cover and Climate Change Scenarios. *Land* **2023**, *12*, 938. https://doi.org/10.3390/land12050938

Academic Editor: Carlos Rogério Mello

Received: 17 March 2023
Revised: 7 April 2023
Accepted: 18 April 2023
Published: 22 April 2023

1. Introduction

The evaluation of the long-term impacts of natural and anthropogenic drivers in catchments constitute social, economic, and environmental dynamics, hydrological processes, contaminant transport, and ecological activities. They also extend to science in all spheres of the environment, which requires an adequate understanding of physiochemical and biophysical responses, environmental problems, monitoring and management policies, economics, data, modeling, and computer capabilities [1–4]. Besides, land use, land cover and climate change are crucial factors that alter the natural environment in due course of time and cause a multitude of impacts on the ecosystem and living conditions. They have notable impacts on hydrologic processes and on the availability, quality, use, and management of freshwater resources [5]. Investigating the impact of climate changes on spatiotemporal fluctuations in regional water resources is an important tool for monitoring the diverse spheres of land, soil, and atmosphere [6]. Shreds of literature from the past two decades have advocated the effectiveness of field sampling, hydrological models, machine learning techniques, artificial intelligence, as well as remote sensing in anticipating land cover and climate change impacts not only at the universal level but also regional and indigenous levels [7–9]. Specifically, hydrological modeling approaches, including numerical, statistical, and conceptual modeling, are widely used to assess the impact of land and climate change on the water resources of catchments [10]. Additionally, the development of

an individual as well as a multitude of scenarios of climate change is of vital use in impact assessment for comparative studies, quality assurance, and reaffirmation of the analyzed scenarios for a tailored study domain [11].

Numerous models have been used to study land and climate changes and their impacts on regional water resources in terms of quantity and quality [12]. A study was conducted to analyze the spatiotemporal dynamics of water fluxes due to climate change in Germany using two models, Statistical Regional (STAR) model and Soil and Water Integrated Model (SWIM). The models were calibrated and validated for the water balance components with high-performance efficiencies (60–90%). The results revealed higher winter flows and lower autumn and summer flows, while the uncertainty of these impacts prevailed [13]. In addition, there were climate change impact assessment studies performed on the Conterminous United States using the Hydrologic Unit Model of the United States (HUMUS), Snake River Planning Model (SRPM), Soil and Water Assessment Tool (SWAT), Regional climate models (RCM), and Global climate models (GCM). The results strongly pointed to the imperative consequences of changing groundwater resources, especially in future climate scenarios [14,15]. Furthermore, studies evaluated the fresh water and groundwater resources considering future climate change that can be utilized for sustainable planning and management of the total water systems using hydro-geological databases [16]. The results revealed that these types of data frameworks could contribute to long-term water resources management and adaptation strategies [17]. However, there are some areas of water resources management needing specific focus in catchment-based climate change assessment studies while accounting for the land use land cover dynamics. They include flood risk and water use investigation associated with development, incorporating industrialization and deforestation effects, and strategizing future water policies [18–20].

Global climate models are a numerical representation of the climate system components that are commonly used for forecasting atmospheric and land surface processes. On the other hand, the regional climate models which are downscaled from GCM focus on limited areas of interest and their dynamics on climate variability. A few studies attempted to quantify the uncertainty in climate projections from GCM on the river catchments and revealed that the changes in the hydrological components of the GCM projections exceed the uncertainty in emission scenarios [21]. Later, various pieces of literature also compared and reviewed the application of RCM and GCM in predicting hydrological components [22]. The findings were complex, ranging from cross-validated severity assessment of droughts using the PRECIS data and GCM, efficient capture of both the timing and amplitude of the hydrological quantities by RCM and GCM, improved seasonal simulations of temperature, precipitation, and stream flows by RCM, as well as a noticeable mismatch in low flow indices [23]. To overcome these limitations, different approaches were implemented to expand the existing study methods with better climate simulations to identify the vulnerable hot spots where significant hydro-geological dynamics occurred with changing climate. They constituted spatially weighted hotspot identification for floods and droughts, crop yield analysis under different climate and management scenarios, and linking GCM simulations and two or more advanced methodologies for enhanced representation of hydrological flows [24,25].

Chennai, one of the most populous urban clusters in India, illustrates the torrential problems of developing countries. The complexities deriving from urban advancements, unequal distribution of wealth, conjunctive and concurrent water uses, supply and demand deficiencies as well as lack of regulatory constraints constitute the capital city of Tamil Nadu State [26]. From a social point of view, Chennai has undergone tremendous changes over the past decade, which elevated the standard of living. However, Chennai paid homage to natural disasters one after the other over the past few years [27]. Proper understanding of the natural resources of Chennai and addressing their degradation with socioeconomic and environmental changes is critical for the self-sustenance of the city in the present and future temporal conditions. Facing diverse environmental and climate change problems, including floods, droughts, and cyclones (1943–2005, 2015, 2017–2018), the sustainability of

water resources in Chennai is a critical issue [28]. Although the governmental strategies for water resources management in the state include the principles of modern water management, strategic aquifers featuring groundwater storage below the city are still being intensively exploited at alarming rates. To add on, the joint effects of socioeconomic and climatic changes worsen groundwater overexploitation which could lead to water quality deterioration [29].

This study aims to assess the potential impacts of land use, land cover and climate change on water resources and water use of catchments primarily located in Chennai in southern India. The prediction advancements in the hydrological responses under land and climate changes, resulting from the implementation of a coupled simulation model, SWAT-FEM, are verified through the study. This study is novel in showcasing the hydro-climatic responses of a catchment under the influence of changing climate using an integrated surface water groundwater model. It serves as an important toolset to achieve successful water governance and agro-industrial practices in Chennai. The study outcomes provide confidence for further application of the model to assess the hydrologic response of regional catchments for land-climate-specific spatial and temporal variability. The remaining sections of this paper are organized as follows: Section 2 lists the materials and methods adopted in this study, Section 3 discusses the results obtained, and Section 4 reports the discussion, followed by Conclusions in Section 5.

2. Materials and Methods

The study aims to evaluate the water resources in the Chennai River catchment using the SWAT-FEM simulation model under present and future land use land cover and climate, as shown in Figure 1. They provide insights into how the variability in climate conditions alters the spatiotemporal hydro-climatic responses in catchment scales. The research methodology adopted to achieve the aim of the study is classified into the following tasks:

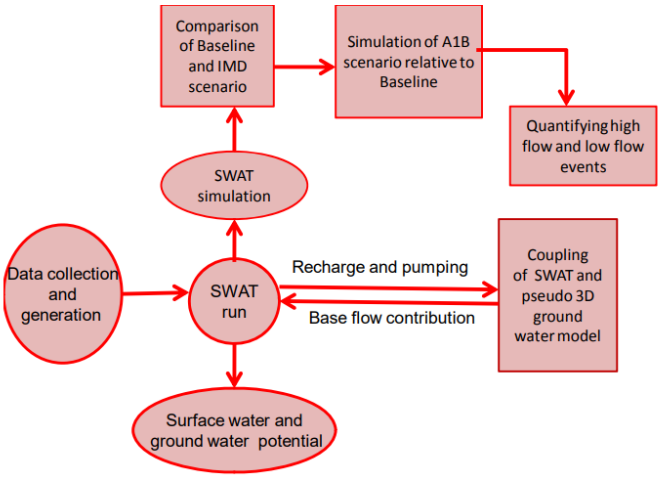

Figure 1. Flowchart of the study methodology.

1. Verification of the effectiveness of SWAT-FEM simulation model for Chennai River catchment.
2. Evaluating climatological responses (precipitation and temperature) under present and future climate conditions.
3. Assessment of hydrological responses (stream flows, groundwater storages, and water use) under present and future climate conditions.

2.1. Study Site

Chennai City is a hydrologically significant coastal zone of the Tamil Nadu state in southern India. The Chennai River catchment, a significant tributary of the state, covers an area of about 6118 km^2. The length of the river catchment is 200 km, and its width varies

from 120 km to 180 km. The maximum elevation and minimum elevation from the mean sea level are 1219 m and 5 m, respectively. The natural ecosystem of Chennai comprises four rivers, five wetlands, and six forest areas. It has several stream networks and reaches out to four districts of Tamil Nadu, namely Thiruvallur, Kancheepuram, Chennai, and Vellore. Adayar, Arainayar, Coovum, and Kosathalayar are the four essential rivers draining the catchment covering areas of 826.517 km^2, 1426.234 km^2, 463.976 km^2, and 3684.274 km^2, respectively, as shown in Figure 2 [30].

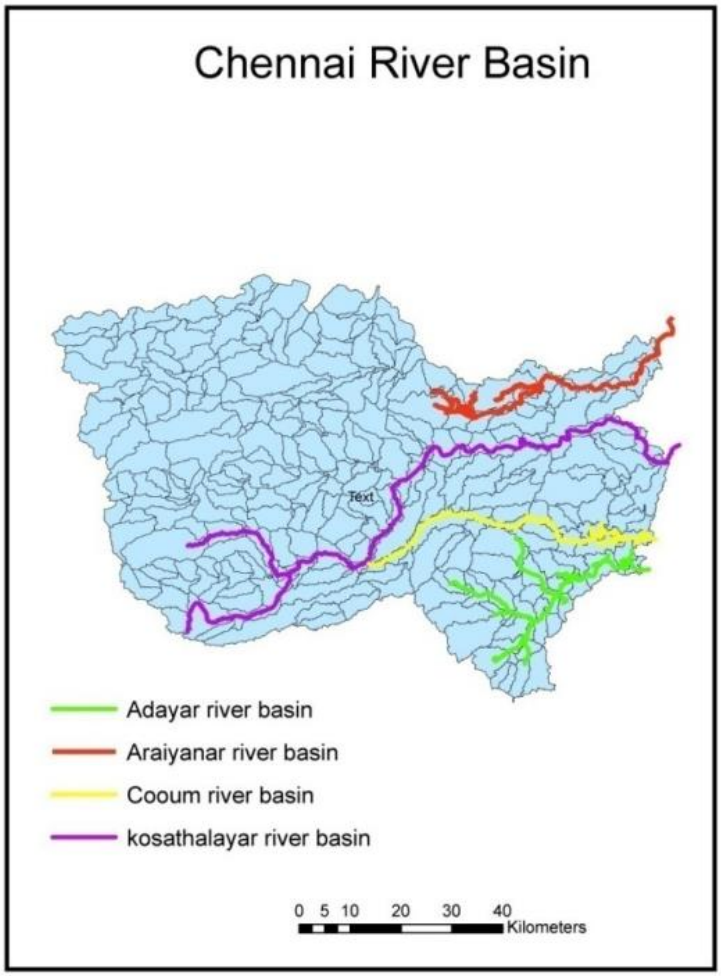

Figure 2. Study area map with the delineated rivers.

2.2. Datasets

The topographic data includes elevation, slope, aspect, flow direction, and flow accumulation. The topographic data for the study were obtained from a digital elevation model (DEM) of the Shuttle Radar Topography Mission (SRTM) with a three-arc second or 90 m resolution. The absolute error and the relative error in the height were less than 16 m and 10 m, respectively [31]. The study used SRTM data because of the averaging operations inherent in the SRTM data. The property of averaging helps in slightly reducing the high-frequency noise inherent in the elevation attributes retrieved from the remotely sensed radars. The soil data mainly included soil texture, soil depth, and soil drainage properties which were obtained from two sources.

For the region of Tamil Nadu, the maps were obtained from the Tamil Nadu Agricultural University (TNAU), Coimbatore, which has a resolution of 1:50,000. The other source is the Food and Agriculture Organization of the United Nations, FAO, with a resolution of 1:10,000,000. FAO maps were used for the northern part of the catchment situated in Andhra Pradesh, where TNAU maps were not available [32,33]. The two maps obtained

for the year 2007 were combined to obtain continuous soil information for the entire study area (Figure 3a).

The model requires meteorological data such as daily precipitation, maximum and minimum air temperatures, solar radiation, wind speed, and relative humidity to simulate the daily hydrological responses. The rainfall observation data sets of the Chennai River catchment were developed by the Indian Meteorological Department (IMD) from 1986 to 2010. The maximum and minimum temperatures used were the 1 deg daily gridded data acquired by the IMD [34]. Solar radiation, relative humidity, and wind speed were simulated using the statistical weather generator (WXGEN) within SWAT using long-term monthly statistics of weather parameters [35].

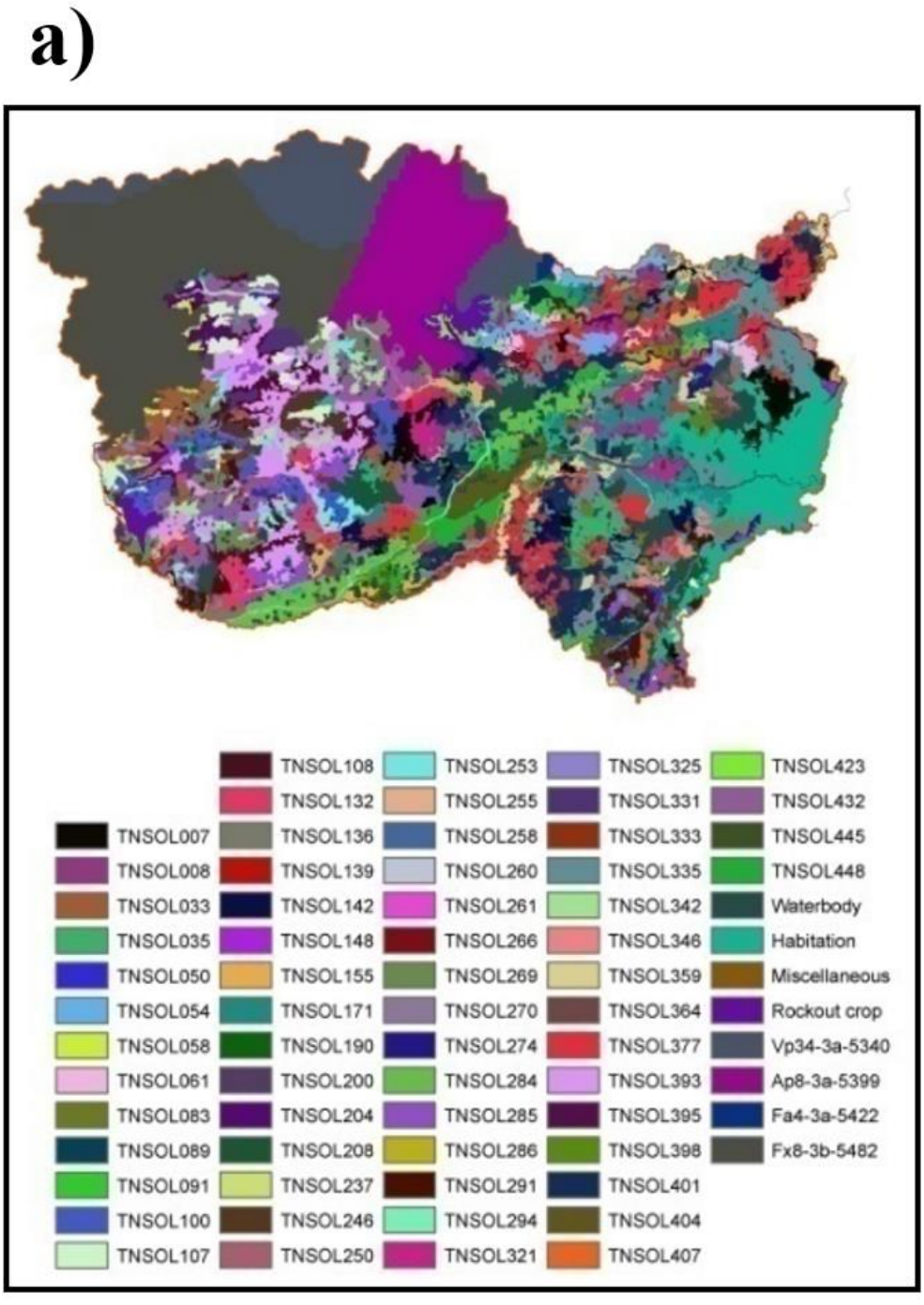

Figure 3. *Cont.*

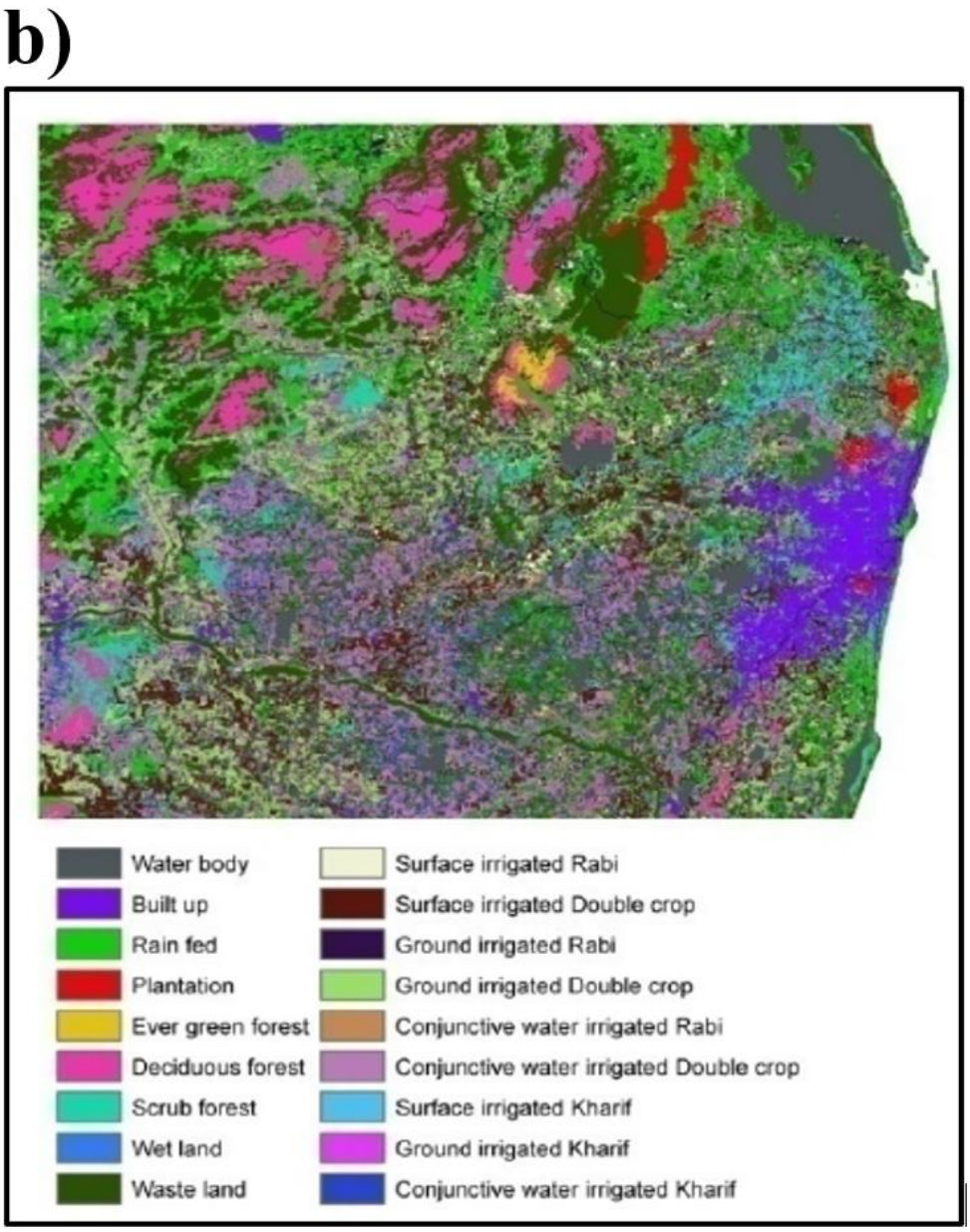

Figure 3. The geospatial representation of (**a**) soil classification and (**b**) land use land cover classification was used in the study.

The historical data was sufficiently available for the periods between 1986 and 2005, which were used as the observed data for calibration and validation of the SWAT-FEM model. This was important to ensure that the model served as a realistic representation of the actual watershed conditions. The historical hydrological data for the study included the stream flows and groundwater levels. These observations were collected from Central Ground Water Board and Global Flood Monitoring System. The SWAT-FEM model simulations were validated with the measured monthly stream flows at the three reservoirs (Poondi, Red Hills, and Chembarambakkam) of the Chennai River catchment from June 1986 to December 2005. These periods were selected for model performance evaluation as the observations during this period were complete and were inclusive of both high-flow and low-flow conditions [30]. The parameters used for calibrating and validating the SWAT-FEM model were the evapotranspiration adjustment factor (ESCO), coefficient of runoff (SURLAG), the fraction of impervious area (A), the upper limit of soil moisture (SOL_ZMX), base flow recession rate (ALPHA_BF), and code of upper limit of groundwater

storage and routing (GWQ_RCO) as indicated in Table 1. The calibration was conducted by force closing the water balance components by taking rainfall versus all surface flow and groundwater components. A trial-and-error process was adopted for calibration, and results yielding the best-fit criteria were followed. These criteria included similarity in the annual or monthly means as well as regression analysis yielding the highest correlation coefficient with a small intercept in the annual regression equation [12]. The most sensitive parameter was found to be ESCO (correlation coefficient, r = 0.67), followed by SURLAG (r = 0.59) and ALPHA_BF (r = 0.55).

Table 1. List of calibration parameters and the optimized values for the SWAT-FEM model.

Parameters	Descriptions	Ranges	Fitted Values
ESCO	evapotranspiration adjustment factor	0.85–1.00	0.920
SURLAG	coefficient of runoff	0–4	2
A	the fraction of impervious area	0–100	26
SOL_ZMX	the upper limit of soil moisture	0–100 mm	50 mm
ALPHA_BF	base flow recession rate	0.10–0.30	0.265
GWQ_RCO	code of upper limit of groundwater storage and routing	0 or 1	0

2.3. Verifying SWAT-FEM Simulation Model

The coupled catchment-scale hydrological model, SWAT-FEM, was used for the catchment modeling and surface water predictions. SWAT classified the catchment domain into several sub-catchments. These sub-catchments were further organized into hydrologic response units having unique soil, unique slope, and unique land use land cover properties. The SWAT model performed steady-state analysis on the temporal extents of years and months and simulated spatially relevant estimates of surface runoff, lateral flow, percolation, and groundwater discharge in the catchment [1]. The FEM model evaluated groundwater storage using the Galerkin finite element method [3,30].

The SWAT-FEM simulation model was employed in this study for generating true surface and subsurface water level predictions under multiple climate change scenarios. The novel model was developed by coupling SWAT with a quasi-3D finite element model (FEM) to overcome the following limitations: (1) The base flow contribution within SWAT uses a simple steady-state approach based on Hooghoudt's equation; (2) The SWAT model considers each sub-catchment units as a separate 1D entity, and hence, the interaction of subsurface flow among them is not simulated. The coupled model assesses the groundwater storage (groundwater below ground level) and base flow contribution realistically, along with the predictions of surface water components. The implementation of the coupled model is expected to elevate the prediction capability of water inflows and outflows in the catchment subjected to present and future scenarios of climate change. The basic concept of coupling is the connection established between the amount of percolation obtained from the SWAT model and the groundwater below the ground level calculated by the FEM model. The percolation is used as the input to FEM, and groundwater below ground level as input to SWAT. The iterations continue until the base flow contribution from SWAT and FEM closely matches following the collected historical values in the catchment (coefficient of determination, R^2 = 0.67). It results in the capture of improved interactions between surface water and groundwater hydrology.

The coupled surface–subsurface flow was simulated with SWAT and a quasi-3D FEM in the study. The synchronized assessment of surface and subsurface responses in the SWAT-FEM simulation model enhanced the representation of interdependent processes of percolation and groundwater storage, which is trivial in the context of land use, land cover, and climate change scenarios (LCS). For the SWAT-FEM modeling of the study, the optimum or suitable gird size (which defines the spatial segmentation of the datasets and the simulations in the study) was obtained using sensitivity analysis of the SWAT-FEM

model. Hence, sensitivity analysis was performed to implement the most suited grid sizing of the SWAT-FEM model in the region of study [36,37].

2.4. Land Use Land Cover and Climate Change Scenarios

The land use land cover data were obtained for the year 2007 from National Remote Sensing Centre (NRSC) developed through the Bhoosampada program at 56 m resolution, and International Water Management Institute (IWMI) developed through Global Irrigated Area Mapping (GIAM) at 500 m resolution. Merging these two datasets were essential because the data from NRSC identified cropping areas based on agricultural seasons but did not have information on irrigation source [38]. The data from GIAM identified cropping areas based on irrigation sources but not the seasons [39]. Hence, for denoting the cropping regions with seasons and sources, the data from both these sources were integrated. For the other areas, land uses land cover information from the high-resolution Bhoosampada data was used to model the hydrology. This combination resulted in the definition of eighteen land use land cover classes with the primary season of production and the source of irrigation water (Figure 3b).

The climate change data used in this study is derived from the Global Climate Model simulations made from Geophysical Fluid Dynamic Laboratory (GFDL) and the Community Climate System Model (CCSM4), downscaled to 25 km × 25 km by the IPRC-RegSIM [40,41]. The GFDL and CCSM4 contain the climate change simulation for the A1B scenario, which refers to the doubling of the CO_2 concentration by the end of the century. The downscaled climate simulations available from IPRC-RegSIM are:

1. GFDL Baseline Scenario (1981–2000)
2. GFDL A1B Scenario (2081–2100)
3. CCSM4 Baseline Scenario (1986–2005)
4. CCSM4 A1B Scenario (2081–2100)

The downscaling of the GCM simulations of the IPCC AR4 scenarios was obtained through the CLIMARICE project by the International Pacific Research Centre (IPRC) Hawaii [42]. The spatiotemporally downscaled weather data available from the climate models include rainfall, temperature, wind speed, relative humidity, and solar radiation. The rainfall and temperature data were bias adjusted using the quantile–quantile mapping technique [43].

2.5. Assessment of Impacts of LCS

2.5.1. Evaluating Land-Climate Responses

The analysis of the input variables, such as rainfall and temperature, was conducted to study the impact of present and future LCS models using unique perspectives [44]. For this, the IMD weather data (1986–2005) was compared to Baseline scenarios and Baseline scenarios to A1B scenarios respectively. The precipitation from the monitored rain gauge stations was collected to analyze the total rainfall coming into the entire Chennai River catchment. The twenty-year averages of the monthly rainfall were estimated to obtain the monthly rainfall of each rain gauge station. Later, the average estimates over the stations were tabulated to obtain the average monthly precipitation over the Chennai River catchment. The same method was adopted to estimate the number of rainy days in a month. A rainy day is one where the rainfall amount realized in a day is 2.5 mm or more [34]. Rainfall intensity is defined as the rainfall per rainy day. It represents the average monthly precipitation per number of rainy days in a month over 20 years. Similarly, the temperature changes in the catchment were also studied using the average monthly temperature estimates over a long-term period of 20 years for IMD, Baseline, and A1B scenarios.

2.5.2. Evaluating Hydrological Responses

The examination of hydrologic response under LCS was performed using the estimates of stream flow hydrographs, flow duration curves, water use estimates, and groundwater

storages [45]. To begin with, flow duration curves and stream flow hydrographs were used to analyze the outflow in the Chennai River catchment over a long-term period of 20 years. A 20-year average was taken to obtain the average monthly and daily flows while maximum and minimum flows were also computed. Later, the average daily flow over the 20 years was taken, and flow duration curves were obtained. Long-term monthly hydrographs and flow duration curves were compared for (1) IMD, Baseline GFDL, and Baseline CCSM4 (2) A1B GFDL and A1B CCSM4. The water use was estimated individually for surface water and groundwater in the study area in IMD and climate change scenarios. Spatial groundwater storage estimates were generated based on a monthly variation of water flows. The seasonality dynamics in groundwater hydrology were understood through the groundwater storage maps of the driest month (February) and the wettest month (November) in India.

3. Results

3.1. Sensitivity Analysis Results of SWAT-FEM Model

To arrive at the most suitable spatial discretization in SWAT-FEM modeling of the study area, a sensitivity analysis was conducted with different grid sizes for a constant time step of one month. The grid size denotes the size of the pixel units of the finite elements to which the catchment is divided using the SWAT-FEM model. The size of each grid was the right-angled sides of the finite triangular elements. The chosen grids were 5 m × 5 m, 10 m × 10 m, 25 m × 25 m, and 50 m × 50 m, and the analysis was carried out for both steady-state as well as unsteady-state conditions. The model runs were carried out to check the convergence of the SWAT-FEM model solution to the analytical solution based on the Dupuits theorem for various time steps [46]. Figure 4a shows the variation of groundwater storage for various grid sizes at different sections of the reach for the aquifer system without recharge. As the size of the grid was reduced from 50 m to 5 m, the accuracy of the model improved. The model solution converged exactly with the analytical solution for the 5 m grid and 10 m grid. The unconfined aquifer with a recharge in Figure 4b also shows the noticeable variation of groundwater storage for different grid sizes at different reach sections. For the system with recharge, the groundwater storage showed further differences with smaller and larger grids compared to the system without recharge. As the size of the grid was reduced from 50 m to 5 m, the accuracy of the model increased significantly. The complete convolution of the model solution with the analytical solution occurred for the smallest grid of 5 m × 5 m. Therefore, the SWAT-FEM model classified the catchment into 5 m × 5 m grids for the hydrological assessments, which depicted the best correlations between modeled and analytical results. Thereafter, the climatic variables of precipitation and temperature were spatially downscaled to represent units of 5 m × 5 m pixels in the catchment [47]. Hence the hydrological simulations conducted based on the variables with the same spatial resolution generated the water balance components for estimating stream flow, groundwater storage, and water use for every 5 m × 5 m pixels in the catchment.

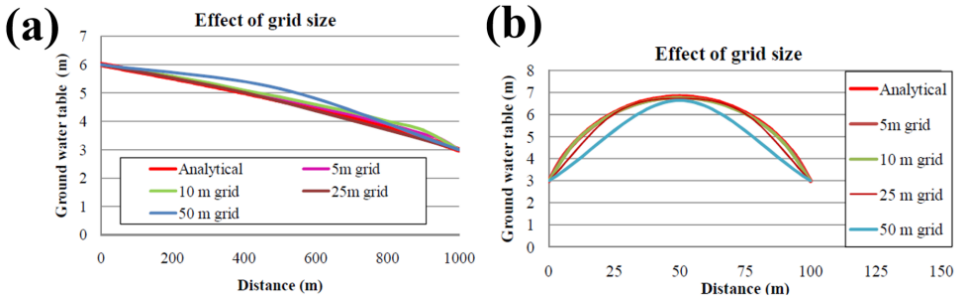

Figure 4. Variation of groundwater levels with different grid sizes for aquifer (**a**) without recharge and (**b**) with a recharge in the catchment.

3.2. Climatic Responses

Table 2 describes the statistics of climate change scenarios used in the SWAT-FEM simulation model. The mean temperature, average rainfall, and the number of rainy days in a month simulated by the GFDL and CCSM4 compared reasonably well with the IMD data, while the future climate scenarios showcased significant positive and negative shifts. The climate data from Baseline scenarios derived from GFDL and CCSM4 models were compared with IMD gridded precipitation and temperature data to understand the uncertainty in the climate simulations.

Table 2. Descriptive statistics of climate change scenarios used in SWAT-FEM model.

Climate Variable	Temperature (°C)		Rainfall (mm)		Rainy Days	
	Minimum	Maximum	Minimum	Maximum	Minimum	Maximum
IMD	24	32	10	183	1	10
Base GFDL	23.6	33.2	43	212	1	11
Base CCSM4	23.3	33.6	42	167	1	9
A1B GFDL	28	33	49.6	343	3	14
A1B CCSM4	26.5	34	16.2	187	2	9

3.2.1. Temperature

Figure 5 displays the long-term average monthly temperatures of the IMD weather data and bias-adjusted Baseline and A1B climate scenarios from GFDL and CCSM4 for the study area during the 20 years. Figure 5a suggests that the monthly temperature (on average 29.42 °C) increases at a rate of 1.71 °C per month between January to May and September to December in IMD and Baseline scenarios. On the other hand, it decreases at a rate of 0.64 °C from May to September. It could be inferred that the Baseline climate conditions from both GFDL and CCSM4 scenarios that exhibited strong similarities in temperature distribution with the IMD gridded data serve as a reliable data source for future climate predictions [48,49]. The seasonal rise and fall patterns are in general agreement with the findings by past researchers, given the bias caused by the difference in the conceptual approaches involved in the three different climate scenarios [50,51]. Figure 5b shows that the long-term average monthly temperature for Baseline GFDL, Baseline CCSM4, A1B GFDL, and A1B CCSM4 as 29.21 °C, 29.36 °C, 31.06 °C, and 30.76 °C respectively. Besides, the average monthly temperature increases in A1B GFDL and A1B CCSM4 were 2.32 °C and 1.74 °C, respectively, compared to their respective Baseline scenarios. It indicates a reasonable closeness in the average monthly temperatures for the present and future scenarios, but in the future, there will be hotter weather. The maximum temperature increases were observed in January (3.11 °C) and December (2.89 °C) for the future climate scenario of A1B GFDL. Unlike the two A1B scenarios, the relatively smaller temperature deviations between the two Baseline scenarios are indicative of the lower inter-month variability in the temperature in the present climate compared to the future climate. These results point to the impacts of an increase in future temperature variability with only a negligible shift of the present temperature trends in the coastal city of Chennai in India. They eventually affect agriculture, crop yields, and surface-ground water interactions, thereby altering the water demands and water supply of Chennai city shortly [51].

3.2.2. Rainfall

Figure 6 depicts the long-term average monthly rainfall, rainy days, and rainfall intensity of the IMD gridded data, as well as the bias-adjusted present and future climate scenarios of GFDL and CCSM4. The maximum deviations in rainfall in Baseline scenarios of GFDL and CCSM4 from IMD were observed in January (30 mm) followed by November. November is the wettest month in the Chennai River catchment with heavy rainfall occurrence from the Northeast (NE) monsoon. Decreasing trends were observed for CCSM4 (15 mm) for November while GFDL (26 mm) showed increasing trends. The trend signifi-

cance patterns while using two different present climate scenarios show the uncertainty in the climate models to predict the NE monsoon [19]. According to the IMD gridded data, October has the maximum number of rainy days, whereas the present climate of GFDL and CCSM4 predicts September to have a greater number of rainy days. As stated before, they throw light on the further improvements that are needed in the climate models to understand the dynamics of the Indian retreating monsoons [52,53]. The analysis showed an insignificant trend of rainfall intensities in the present and future climate. The rainfall intensity tends to increase in the A1B GFDL scenario, and maximum rainfall intensity is expected in November. However, A1B CCSM4 predictions show a reduction in the intensity of rainfall in future climatic conditions. Therefore, improved precipitation data within climate change scenarios with excellent and consistent prediction capacity on micro scales is a requisite to understanding the impacts of climate variability on social, economic, and environmental vulnerability [54].

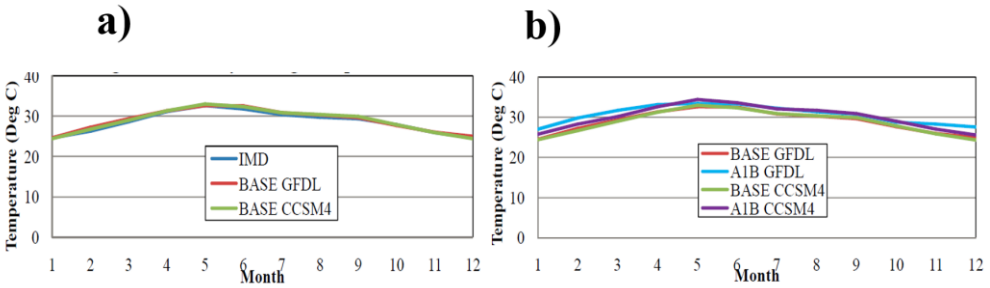

Figure 5. Long-term mean monthly temperatures over a 20-year period in the study area for (**a**) IMD and Baseline scenarios and (**b**) Baseline and A1B scenarios.

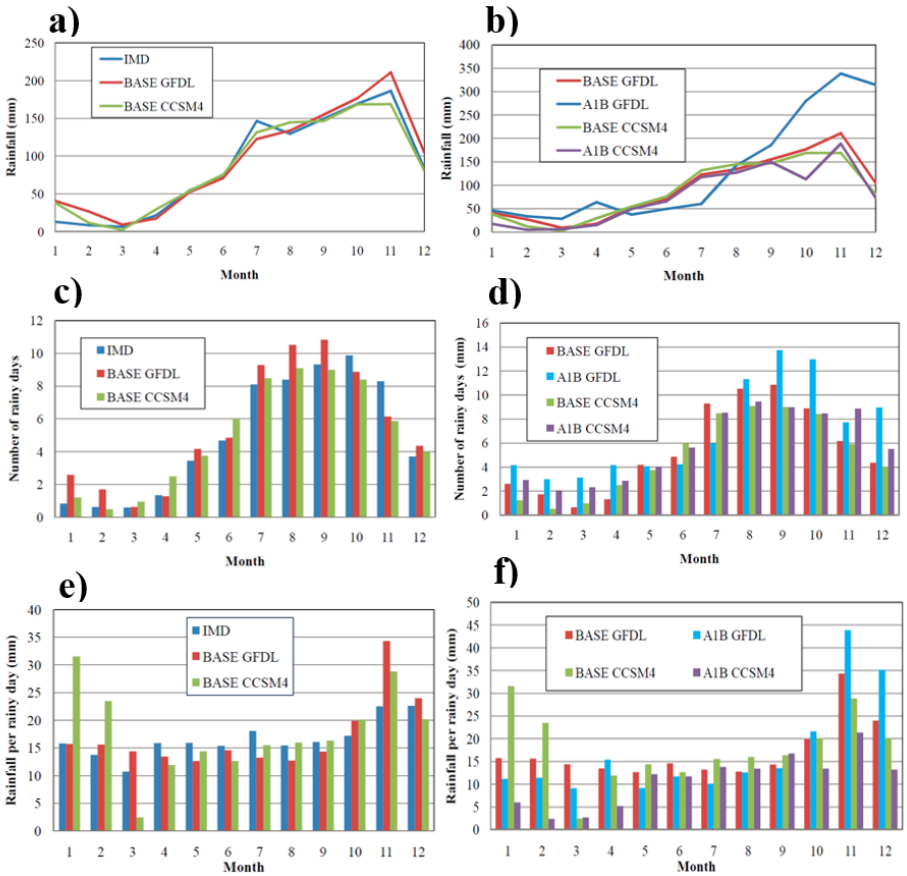

Figure 6. Long-term mean monthly estimates of rainfall (**a**,**b**), rainy days (**c**,**d**), and rainfall intensity (**e**,**f**) over a 20-year period in the study area for IMD, Baseline and A1B scenarios.

3.3. Hydrological Responses

The impact of climate change scenarios on the hydrological processes, such as stream flows, flow duration curves, groundwater storage, and water use in Chennai River, was ascertained.

3.3.1. Stream Flows

Figure 7 outlines the projected changes in monthly stream flows concerning the baseline climate under A1B scenarios. In both A1B scenarios, the average monthly stream flows were projected to increase at the four sub-catchments of the study area [55]. However, the A1B simulations with GFDL climate data predicted much higher flow volumes compared to A1B CCSM4. This is an indication of the uncertainty of GFDL and CCSM4 climate change models in simulating the future climate for the same emission scenario of A1B [21,52]. The stream flow increases in the A1B GFDL scenario (ranging from 25 cumecs to 50 cumecs) were noticeably higher than that of A1B CCSM4 (ranging from 2 cumecs to 20 cumecs), especially for NE monsoon. The increased future stream flows in NE monsoon could be due to less accumulation of snowfall that would result from the decreased intensity of rainy days in NE monsoon. This is based on the assessments in Figure 6 that indicate that precipitation will decrease in NE monsoon compared to Southwest (SW) monsoon while they increase in spring. Conversely, decreased stream flows were predicted for July and August in A1B GFDL and for January and February in A1B CCSM4, respectively. It was interesting to note that no projected variations were observed for the summer months of March and April at all sub-catchments and under both scenarios. This contrasts with the research showcasing the weakening of precipitation events and stream flow in the Indian summers [56,57]. Overall, the projected stream flow changes in this study appear more important than the projected changes in precipitation. This could be because of the non-inclusion of the factors of atmospheric deposition, snow cover, and annual land use land cover variations, as well as the theoretical approach in rainfall estimation, which inbuilt into the SWAT-FEM model [14]. To add on, the increase in mean stream flow under both future scenarios ratifies the increasing temperature patterns in the catchment [58]. Overall, the mean monthly stream flows were projected to increase by 21–25% by the end of the century in the Chennai River under A1B scenarios from GFDL and CCSM4.

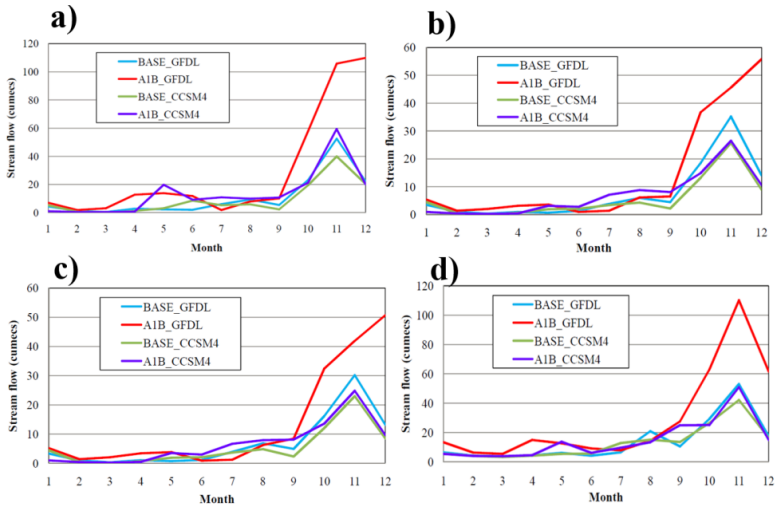

Figure 7. Projected monthly streamflow estimates (cumecs) of climate change scenarios for Chennai River catchment at the sub-catchment outlets of (**a**) Kosthalayar, (**b**) Adayar, (**c**) Coovum and (**d**) Arainayar.

3.3.2. Flow Duration Curves

The flow duration curves clearly show that the stream flows are going to be generally higher in the A1B scenario when compared to the current conditions. This is because

rainfall is predicted to be higher during the A1B scenario. Flow predictions with the GFDL data for the A1B scenario suggest a much higher stream flow than those predicted with CCSM4 data. This indicates the uncertainty among the climate models in predicting the Indian monsoon.

Figure 8 displays the analogy of flow duration curves during the baseline periods and the future periods under A1B scenarios at the four sub-catchments of the Chennai River catchment. The results show that the probability of occurrence of flow and magnitudes of flow could be higher in the future in the study area under both scenarios. In this analysis, high flows are depicted by 10% exceedance (S10), medium flows by 60% exceedance (S60), and low flows by 95% exceedance (S95) under all scenarios. Under the A1B GFDL scenario, high flows and medium flows were projected to increase spatially for the catchment, with the ranges 12–32% (S10) and 8–54% (S60), respectively. This is in conformance with the increases in average monthly estimates of rainfall and temperature in the basin, as illustrated in Figures 5 and 6. However, notable estimates of S95 were only predicted in the sub-catchment of Arainayar by A1B GFDL and were found to decrease by 21% in the future. This signifies the importance of spatial heterogeneity of water flows and their temporal dynamics in addressing the uncertainty in the sub-basin scale stream flow predictions within the Chennai River catchment for climate change impact assessments [19]. On the other hand, flow duration curves for the A1B CCSM4 scenario projected fewer positive deviations from Baseline CCSM4 (0–8% for S10 and 2–20% for S60) compared to the GFDL scenarios in present and future averaged for the catchment. Despite the closeness between the two present climate scenarios, two future climate scenarios that were developed using the same emission approach predicted differing flow magnitudes, all of which can affect the quantification of stream flow responses using future climate change models [59].

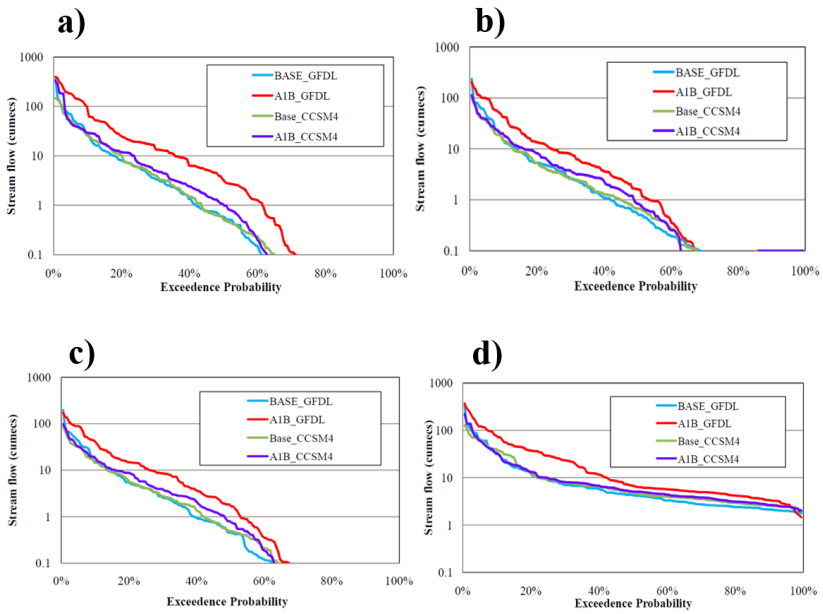

Figure 8. Projected monthly stream flow duration curves of climate change scenarios for Chennai River catchment at the sub-catchment outlets of (**a**) Kosthalayar, (**b**) Adayar, (**c**) Coovum and (**d**) Arainayar.

3.3.3. Groundwater Storage

The spatial groundwater storage estimates of the catchment were developed using the monthly average groundwater below ground levels (GWBGL), obtained from the SWAT-FEM model. They were compared for the Baseline scenarios and A1B scenarios from both models for the managed conditions of the watershed. The spatial distribution of the GWBGL in the four sub-catchments of the Chennai River catchment was reported for the driest month of February (Figure 9) and the wettest month of November (Figure 10) to

scrutinize the seasonal variability of climate change impacts on groundwater hydrology [60]. The groundwater storage is expected to increase in A1B GFDL concerning Baseline GFDL, whereas it is predicted to decrease in A1B CCSM4 concerning Baseline CCSM4. These conflicting results indicate the importance of more accurate predictions in the distribution of rainfall. This is because the number of rainy days and hence rainfall intensities during the rainy days are estimated to be quite different, although both models show similar rainfall predictions (Figure 6). Spatially, the variability in groundwater storages was majorly observed in the northwestern portion of Chennai River comprising Kosthalayar and Arainayar sub-catchments by the end of the century in both scenarios. The results show that the spatial distribution of the groundwater storage is not affected much by climate change according to the model predictions (0–0.89 m), except for the northwest of the Chennai River catchment (0.50–2.49 m). However, the most distinctive is a conflicting trend of the future groundwater storage predictions from two climate change models of GFDL and CCSM4 [61]. We recommend a smart selection of climate change models tailored to the most favorable downscaling method/methods for the area of study. Such results are expected to enhance future groundwater predictions for coastal regions such as Chennai, where groundwater serves as the main source of water supply. Additionally, the study results make it apparent that the long-term monthly rainfall distribution has a major influence on the evolution of the groundwater system [62].

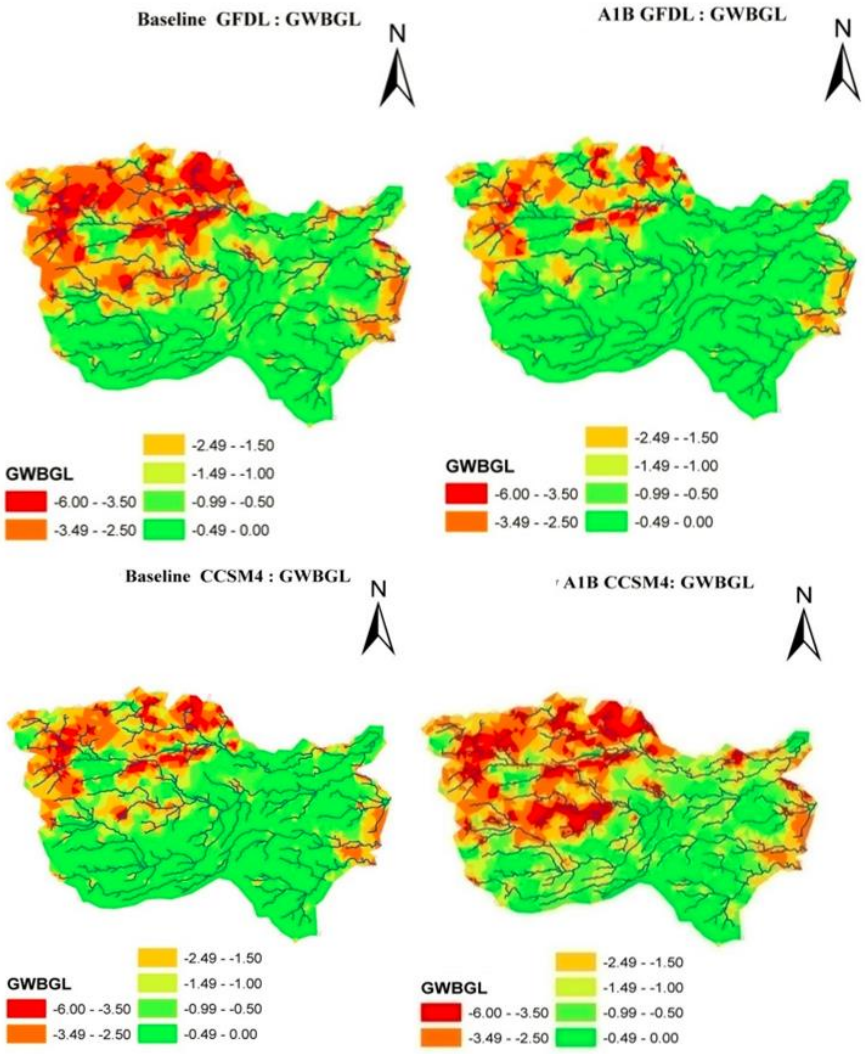

Figure 9. Projected groundwater levels in climate change scenarios for Chennai River catchment for the month of February.

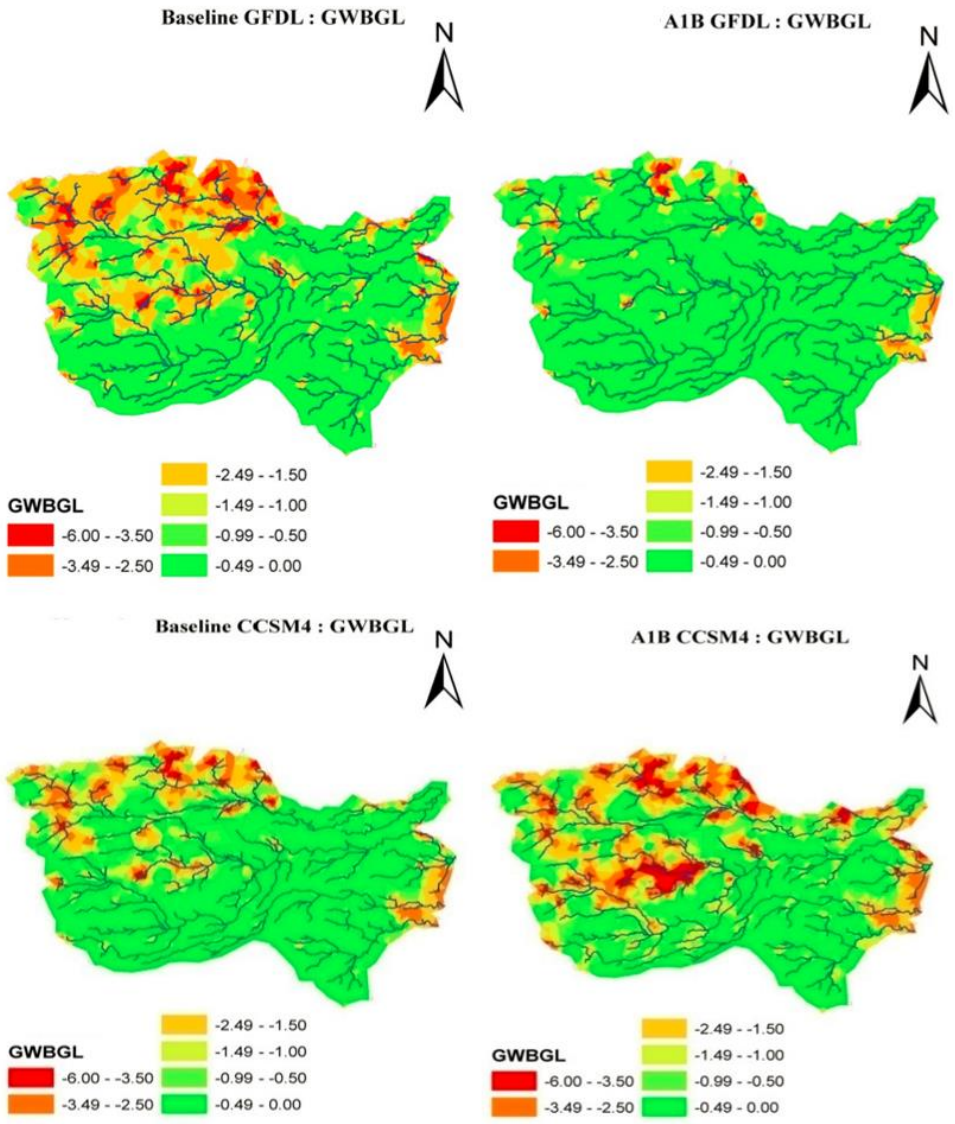

Figure 10. Projected groundwater levels in climate change scenarios for Chennai River catchment for the month of November.

3.3.4. Water Use

The total water use in the catchment primarily constitutes surface water use and groundwater use. It is calculated in the study as:

$$\text{Water use} = \text{Surface water use} + \text{Groundwater use} \quad (1)$$

$$\text{Water use} = \text{Surface runoff} + \text{Lateral flow} + \text{Base flow} + \text{Percolation} - \text{Groundwater discharge} \quad (2)$$

The impacts of climate change scenarios on water use were evaluated using relative changes in water use between Baseline and A1B conditions from two different climate change scenarios (Table 3). The monthly water use was greatest in November and least in March under all four climate change scenarios in the catchment. The annual water use of the study area is expected to be 51.23% higher in A1B GFDL concerning Baseline GFDL. From the GFDL predictions, it could be noted that more water use is expected to happen by the end of the century. This also demonstrates the non-adequacy of the available water resources and the possibilities of regional groundwater extraction soon [63].

Table 3. Monthly water use predictions and annual water use statistics in Chennai River catchment with four climate change scenarios.

Month	Water Use (mm)				Variability (mm)	
	Base GFDL	**A1B GFDL**	**Base CCSM4**	**A1B CCSM4**	**GFDL**	**CCSM4**
1	21.17	35.86	24.73	4.64	14.69	−20.09
2	5.28	8.10	2.29	1.16	2.82	−1.13
3	0.09	6.92	−0.72	0.70	6.83	1.42
4	6.78	36.55	5.29	5.07	29.77	−0.22
5	10.40	30.66	14.09	39.53	20.26	25.44
6	7.85	12.66	17.87	19.02	4.81	1.15
7	26.25	10.88	35.18	40.14	−15.37	4.96
8	66.04	43.04	43.97	46.32	−23.00	2.35
9	34.65	83.16	30.15	69.90	48.51	39.75
10	115.10	238.90	97.13	58.52	123.80	−38.61
11	208.60	359.03	161.58	202.87	150.43	41.29
12	87.87	345.20	60.68	61.47	257.33	0.79
Water Use Statistics						
Water use		Base GFDL	A1B GFDL	Base CCSM4	A1B CCSM4	
Annual		590.08	1210.96	492.24	549.34	
Mean		49.17	100.91	41.02	45.78	
Standard deviation		62.092	133.369	46.9777	55.4549	

4. Discussion

4.1. Impacts of LCS on Water Resources and Regional Watersheds

Overall, the variability of water use in the Chennai River catchment is extensive, along with shreds of evidence of divergent trends under the climate change scenarios. This is seconded by the monthly water use variability ranging from −23 mm to 620 mm and −39 mm to 57 mm for GFDL and CCSM4, respectively. This indicates the significant seasonal variability of the water yields from surface and ground in the catchment scale, projected because of climate change impact assessment with the sole use of two climate change models [59,61]. Overall, the water use predictions suggested increases above 20% in the utilization of water by the end of the century, except for August (2.1%). On the contrary, the low variability in water yields in March was increased slightly under CCSM4 as well as under GFDL, indicating the satisfactory water balance naturally maintained in the coastal region, making them less prone to unjustified water extraction [64]. In terms of inter-annual variability, the highest differences were observed for the future A1B scenarios compared to the Baseline scenarios. The annual water use of the catchment was found to be the least variable in the Baseline CCSM4, whereas A1B GFDL exhibited the most significant variations (Table 3). The results infer that climate change results in noticeable dynamics of inter-annual as well as inter-month variability in water utilization in the river basins of Chennai [40].

As land-climate change is a complex phenomenon, it is tough to comprehensively assess climate change impacts on surface water and groundwater spatially and temporally. Various shreds of the literature indicated that GFDL scenarios are a good predictor of temperature for the Asian continent, where climate change had profound effects over the last two decades. However, the GFDL scenario is found to be a less likely predictor of precipitation effects and their geostatistical trends for future climate conditions [65,66]. Some of the past research compared different global climate models using their representative concentration pathways. They highlighted that GFDL and CCSM4 models provide optimal performance for temperature and precipitation changes in annual and inter-annual time frames for African watersheds. These studies emphasized that urban environments should be the focus of climate change projection for effective water resources management.

Recent studies remarked that CCSM4 simulations provide reasonable predictions in the secular Arctic climate domains where greenhouse forcing and significant land and climate sensitivity prevail [67].

4.2. Limitations and Challenges

Although our SWAT-FEM model was able to capture the observed differences in stream flows, there was some disagreement in their spatial predictions [68,69]. The limitations of the study, which may alter hydro-climatological responses of the projected results of the study, are as follows:

(1) The spatial and temporal resolution of the observed data (daily) and the modeled predictions (monthly) might be inconsistent.
(2) The groundwater flow and all the geologic formations are assumed to be horizontal.
(3) The prediction of future hydrological responses of stream flows, groundwater storage, and water use did not capture the dynamics of the annual land use land cover variations in the basin from 2081 to 2100.
(4) The confounding point and non-point sources of pollution in the future are not considered.

Some of the difficulties encountered in adopting the study methodology and analysis are as follows:

(1) The temporal spans of the four climate change scenarios (20 years) put forth some biases for long-term evaluation of climate change effects in surface and ground hydrology.
(2) The implementation of suitable policies for cognizing climate change impacts demands extensive calibration and validation of the study models to adopt the best management practices in the study area [70].

Specifically, for the study area, we recommend further assessments using multiple GCMs with an A1B scenario to overcome the existing biases in hydrological and climatological predictions, which can uncover new horizons of impacts of climate change on water resources in the basin. Besides, the existing biases of the climatological response of rainfall and the hydrological response of stream flows by the future climate change models pinpoint the need for a merger of climate change models, including several emission scenarios in arriving at reliable hydro-climatic responses in river basins.

5. Conclusions

This study implemented a coupled surface–subsurface flow model and evaluated the impacts of climate change on the water resources of the Chennai River catchment in India. The Soil and Water Assessment Tool and quasi 3D finite element model were combined to form the coupled model, SWAT-FEM simulation model. The synchronized assessment of surface and subsurface responses in the SWAT-FEM simulation model enhanced the representation of interdependent processes of percolation and groundwater storage, which is very important in climate change studies. Climate change simulations were obtained from four global climate models, including GFDL Baseline Scenario (1981–2000), GFDL A1B Scenario (2081–2100), CCSM4 Baseline Scenario (1986–2005), and CCSM4 A1B Scenario (2081–2100) by bias adjustments using the quantile–quantile mapping technique. The hydro-climatic responses, including precipitation, temperature, stream flows, groundwater storage, and water use, were assessed under present (Baseline GFDL and Baseline CCSM4) and future (A1B GFDL and A1B CCSM4) climate change scenarios. The average monthly temperature increases in A1B GFDL and A1B CCSM4 were 2.32 °C and 1.74 °C, respectively, compared to their respective Baseline scenarios. For the climatic change scenarios considered, significant increases were expected in the monthly stream flows (21–25%) and less spatial variation in the groundwater storages (0–0.89 m) by 2100. Spatially, the variability in groundwater storages was majorly observed in the northwestern portion of Chennai River, comprising Kosthalayar and Arainayar sub-catchments, by 2100. Overall, the water

use predictions suggested increases above 20% in the utilization of water by the end of the century. It is inferred that the future climate is projected to produce noticeable dynamics of inter-annual as well as inter-month variability in water resources in the river basins of Chennai.

The uncertainties associated with the study findings include (1) overpredicted rainfall estimates of present scenarios of GFDL and CCSM4 for NE monsoon compared to IMD, (2) underpredicted monthly stream flow predictions of future scenarios of GFDL and CCSM4 compared to IMD, and (3) over predictions of monthly flow duration curves for the future scenario of GFDL compared to CCSM4. While these uncertainties in the predictions of hydrological responses using a minimal number of climate change scenarios are limiting, a smart selection of multiple regional climate change scenarios suited to the study area and its surface water hydrology is recommended. The study uncertainty is mainly attributed to the use of multiple climate change scenarios from different temporal extents, emission parameters, and concentration pathways. Besides, the resolution of the data used, such as land, soil, and digital elevation model, could act as confounding variables in causing uncertainty in the hydrologic responses of the study. In general, the unique implementation of a coupled modeling approach improved the practicality of the simulation model and delivered useful projections of climate change impacts on hydro-climatic responses. These outcomes provide useful insights into how the variability in land and climate conditions alters the spatiotemporal hydro-climatic responses in catchment and sub-catchment scales. The study contributes to the further application of the developed model to assess the hydrologic response of regional catchments for land-climate-specific spatial and temporal variability.

Author Contributions: Conceptualization, P.P.; methodology, P.P.; software, P.P.; validation, M.H. and P.P.; formal analysis, M.H.; writing—review and editing, P.P. and M.H. All authors have read and agreed to the published version of the manuscript.

Funding: This research received no external funding.

Data Availability Statement: Data will be available upon request.

Acknowledgments: I would like to acknowledge the editors and reviewers for improving the article.

Conflicts of Interest: The authors declare no conflict of interest.

References

1. Arnold, T.R. Procedural knowledge for integrated modelling: Towards the modelling playground. *Environ. Model Softw.* **2013**, *39*, 135–148. [CrossRef]
2. Laniak, G.F.; Olchin, G.; Goodall, J.; Voinov, A.; Hill, M.; Glynn, P.; Hughes, A. Integrated environmental modeling: A vision and roadmap for the future. *Environ. Model Softw.* **2013**, *39*, 3–23. [CrossRef]
3. Joseph, N.; Preetha, P.P.; Narasimhan, B. Assessment of environmental flow requirements using a coupled surface water-groundwater model and a flow health tool: A case study of Son river in the Ganga basin. *Ecol. Ind.* **2021**, *121*, 107110. [CrossRef]
4. Preetha, P.P.; Al-Hamdan, A.Z. Multi-level pedotransfer modification functions of the USLE-K factor for annual soil erodibility estimation of mixed landscapes. *Model. Earth Syst. Environ.* **2019**, *5*, 767–779. [CrossRef]
5. Preetha, P.P.; Al-Hamdan, A.Z.; Anderson, M.D. Assessment of climate variability and short term land use land cover change effects on water quality of Cahaba river basin. *Int. J. Hydrol. Sci. Technol.* **2019**, *11*, 54. [CrossRef]
6. Gosain, A.K.; Rao, S.; Basuray, D. Climate change impact assessment on hydrology of Indian river catchments. *Curr. Sci.* **2006**, *90*, 346–353.
7. Jylhä, K.; Fronzek, S.; Tuomenvirta, H.; Carter, T.R.; Ruosteenoja, K. Changes in frost, snow and Baltic Sea ice by the end of the twenty-first century based on climate model projections for Europe. *Clim. Chang.* **2008**, *86*, 441–462. [CrossRef]
8. Preetha, P.P.; Al-Hamdan, A.Z. A union of dynamic hydrological modeling and satellite remotely-sensed data for spatiotemporal assessment of sediment yields. *Remote Sens.* **2022**, *14*, 400. [CrossRef]
9. Preetha, P.P.; Al-Hamdan, A.Z. Synergy of remotely sensed data in spatiotemporal dynamic modeling of the crop and cover management factor. *Pedosphere* **2022**, *32*, 381–392. [CrossRef]
10. Brouyère, S.; Carabin, G.; Dassargues, A. Climate change impacts on groundwater resources: Modelled deficits in a chalky aquifer, Geer basin, Belgium. *Hydrogeol. J.* **2004**, *12*, 123–134. [CrossRef]
11. Almazroui, M. Temperature variability over Saudi Arabia during the period 1978–2010 and its association with global climate indices. *J. King Abdulaziz Univ. Met Env. Arid. Land Agric. Sci.* **2012**, *23*, 85–108. [CrossRef]

12. Kim, N.W.; Chung, M., II; Won, Y.S.; Arnold, J.G. Development and application of the integrated SWAT-MODFLOW model. *J. Hydrol.* **2008**, *356*, 1–16. [CrossRef]
13. Huang, S.; Krysanova, V.; Osterle, H.; Hattermann, F.F. Simulation of spatiotemporal dynamics of water fluxes in Germany under climate change. *Hydrol. Process.* **2010**, *24*, 3289–3306. [CrossRef]
14. Eckhardt, K.; Ulbrich, U. Potential impacts of climate change on ground water recharge and streamflow in a central European low mountain range. *J. Hydrol.* **2003**, *284*, 244–252. [CrossRef]
15. Pulido-Velazquez, M.; Peña-Haro, S.; García-Prats, A.; Mocholi-Almudever, A.F.; Henriquez-Dole, L.; Macian-Sorribes, H.; Lopez-Nicolas, A. Integrated assessment of the impact of climate and land use changes on groundwater quantity and quality in the Mancha Oriental system (Spain). *Hydrol. Earth Syst. Sci.* **2015**, *19*, 1677–1693. [CrossRef]
16. Kingston, D.G.; Taylor, R.G. Sources of uncertainty in climate change impacts on river discharge and groundwater in a headwater catchment of the Upper Nile Basin, Uganda. *Hydrol. Earth Syst. Sci.* **2010**, *14*, 1297–1308. [CrossRef]
17. Jha, M.; Arnold, J.G.; Gassman, P.W.; Gu, R. Climate change sensitivity assessment on Upper Mississippi River Catchment streamflows using SWAT. Center for Agricultural and Rural Development Iowa State University Ames, Iowa. *J. Am. Water Resour. Assoc.* **2004**, *42*, 50011–51070.
18. Hoekema, D.J.; Jin, X.; Sridhar, V. Climate change and the Payette river catchment. *Collab. Manag. Integr. Catchments* **2010**, 1053–1067.
19. Ghosh, S.; Das, D.; Kao, S.C.; Ganguly, A.R. Lack of uniform trends but increasing spatial variability in observed Indian rainfall extremes. *Nat. Clim. Chang.* **2012**, *2*, 86–91. [CrossRef]
20. Zhang, R.; Srinivasan, F.H. Predicting hydrologic response to climate change in the Luohe River Catchment using the SWAT model. *Am. Soc. Agric. Biol. Eng.* **2007**, *50*, 901–910.
21. Xu, H.; Taylor, R.G.; Xu, Y. Quantifying uncertainty in the impacts of climate change on river discharge in sub-catchments of the Yangtze and Yellow River Basins, China. *Hydrol. Earth Syst. Sci.* **2011**, *15*, 333–344. [CrossRef]
22. Takle, E.S.; Jha, M.; Lu, E.; Arritt, R.W.; Gutowski, W.J. Streamflow in the upper Mississippi river catchment as simulated by SWAT driven by 20th century contemporary results of global climate models and NARCCAP regional climate models. *Meteorol. Z.* **2010**, *19*, 341–346. [CrossRef]
23. Nagraj, S.; Patil, A.; Gosain, K. GIS framework to evaluate the impact of climate change on water resources. *Curr. Sci.* **2011**, *101*, 3.
24. Lakshmanan, V.; Geethalakshmi, R.; Sekhar, S.N.U.; Annamalai, H. Climate change adaptation strategies in Bhavani basin using SWAT model. *J. Appl. Eng. Agric.* **2011**, *27*, 887–893. [CrossRef]
25. Nourani, V.; Rouzegari, N.; Molajou, A.; Baghanam, A.H. An integrated simulation-optimization framework to optimize the reservoir operation adapted to climate change scenarios. *J. Hydrol.* **2020**, *587*, 125018. [CrossRef]
26. Sivaraman, K.R.; Thillaigovidarajan, S. Chennai River Basin Micro Level Report. 2012. Available online: http://www.rainwaterharvesting.org (accessed on 22 November 2012).
27. Nair, M.R.; Ramya, G.R.; Sivakumar, P.B. Usage and analysis of Twitter during 2015 Chennai flood towards disaster management. *Procedia Comput. Sci.* **2017**, *115*, 350–358. [CrossRef]
28. Shanmugam, P.; Neelamani, S.; Yu-Hwan, A.; Philip, L.; Gi-Hoon, H. Assessment of the levels of coastal marine pollution of Chennai city Southern India. *Water Resour. Manag.* **2007**, *21*, 187–1206. [CrossRef]
29. Jayaprakash, M.; Urban, B.; Velmurugan, P.M.; Srinivasalu, S. Accumulation of total trace metals due to rapid urbanization in microtidal zone of Pallikaranai marsh, South of Chennai, India. *Environ. Monit. Assess.* **2010**, *170*, 609–629. [CrossRef]
30. Preetha, P.P.; Joseph, N.; Narasimhan, B. Quantifying surface water and groundwater interactions using a coupled SWAT_FEM model: Implications of management practices on hydrological. *Water Resour. Manag.* **2021**, *35*, 2781–2797. [CrossRef]
31. CGIARCSI. Data from: SRTM 90m DEM. SRTM 90m Digital Elevation Database v4.1: Consortium for Spatial Information (CGIARCSI). 2018. Available online: http://www.cgiar-csi.org/data/srtm-90m-digital-elevation-database-v4-1 (accessed on 15 June 2018).
32. TNAU. Data from: TNAU Agritech Portal: Downloads. Tamil Nadu Agricultural University, Coimbatore. 2018. Available online: http://agritech.tnau.ac.in/downloads.html (accessed on 3 March 2018).
33. FAOSTAT. Data from: Soil data 2007. The Food and Agriculture Organization of the United States (FAO) Database. 2018. Available online: http://www.fao.org/faostat/en/#data (accessed on 15 April 2018).
34. Indian Meteorological Department. Data from: Meteorological Centre: Season's Rainfall. IMD: Season's Rainfall 1986–2010 Meteorological Centre, Tamil Nadu. 2018. Available online: https://imdtvm.gov.in/index.php?option=com_content&task=view&id=29&Itemid=43 (accessed on 15 March 2023).
35. Green, C.H.M.; Griensven, A. Autocalibration in hydrologic modeling: Using SWAT2005 in small-scale catchments. *Environ. Model. Softw.* **2018**, *23–24*, 422–434.
36. Preetha, P.P.; Johns, M. A review of recent water quality assessments in watersheds of southeastern United States using continuous time models. *Global J. Eng. Sci.* **2022**, *9*, 1–4. [CrossRef]
37. Preetha, P.P.; Maclin, K. Evaluation of Hydrogeological Models and Big Data for Quantifying Groundwater Use in Regional River Systems. In *Environmental Processes and Management. Water Science and Technology Library*; Shukla, P., Singh, P., Singh, R.M., Eds.; Springer: Cham, Germany, 2023; Volume 120. [CrossRef]
38. NRSC. Data from: Geophysical Products/Land Products. Indian Space Research Organization: Natural Remote Sensing Centre (NRSC) Database. 2018. Available online: https://nrsc.gov.in/Geophysical_Products (accessed on 17 May 2018).

39. IWMI. Data from: Land Products. International Water Management Institute (IWMI): Global Irrigated Area Mapping (GIAM) Database. 2018. Available online: http://www.iwmi.cgiar.org/ (accessed on 18 May 2018).
40. Annamalai, H.; Hamilton, K.; Sperber, K.R. South Asian Summer Monsoon and its relationship with ENSO in the IPCC AR4 simulations. *J. Clim.* **2007**, *20*, 1071–1092. [CrossRef]
41. Meehl, G.; Arblaster, J.; Caron, J.; Annamalai, H.; Jochum, M.; Chakraborty, A.; Murtugudde, R. Monsoon regimes and processes in CCSM4, Part 1: The Asian-Australian monsoon. *J. Clim.* **2012**, *25*, 2583–2608. [CrossRef]
42. Balasubramanian, R.; Saravanakumar, V.; Boomiraj, K. Chapter 4-Ecological Footprints of and Climate Change Impact on Rice Production in India. In *The Future Rice Strategy for India*; Elsevier: Amsterdam, The Netherlands, 2017; pp. 69–106.
43. Sperber, K.R.; Annamalai, H.; Kang, I.-S.; Kitoh, A.; Moise, A.; Turner, A.; Wang, B.; Zhou, T. The Asian Summer Monsoon: An Intercomparison of CMIP5 vs. CMIP3 Simulations of the Late 20th Century. *Clim. Dyn.* **2013**, *41*, 2711–2744. [CrossRef]
44. Rao, K.P.C.; Ndegwa, W.G.; Kizito, K.; Oyoo, A. Climate variability and change: Farmer perceptions and understanding of intra-seasonal variability in rainfall and associated risk in semi-arid Kenya. *Exp. Agric.* **2011**, *47*, 267–291. [CrossRef]
45. Miles, E.L.; Snover, A.K.; Hamlet, A.F.; Callahan, B.; Fluharty, D. Pacific Northwest Regional Assessment: The Impacts of Climate Variability and Climate Change on the Water Resources of the Columbia River Basin. *J. Am. Water Resour. Assoc. JAWRA* **2000**, *36*, 399–420. [CrossRef]
46. Mishra, P.K.; Kuhlman, K.L. Unconfined aquifer flow theory: From Dupuit to present, chap 9. In *Advances in Hydrogeology*; Springer: Heidelberg, Germany, 2013; pp. 185–202.
47. Maurer, E.P.; Hidalgo, H.G. Utility of daily vs. monthly large-scale climate data: An intercomparison of two statistical downscaling methods. *Hydrol. Earth Syst. Sci.* **2008**, *12*, 551–563. [CrossRef]
48. Dixon, K.W.; Delworth, T.; Knutson, T.; Spelman, M.; Stouffer, R. A comparison of climate change simulations produced by two GFDL coupled climate models. *Glob. Planet. Change* **2003**, *37*, 81–102. [CrossRef]
49. Delworth, T.; Stouffer, R.; Dixon, K.; Spelman, M.; Knutson, T.; Broccoli, A.; Kushner, P.; Wetherald, R. Review of simulations of climate variability and change with the GFDL R30 coupled climate model. *Clim. Dyn.* **2002**, *19*, 555–574.
50. Wasko, C.; Sharma, S.A. Westra Reduced spatial extent of extreme storms at higher temperatures. *Geophys. Res. Lett.* **2016**, *43*, 4026–4032. [CrossRef]
51. Sharma, A.; Wasko, D.P.C. Lettenmaier If precipitation extremes are increasing, why aren't floods? *Water Resour. Res.* **2018**, *54*, 8545–8551. [CrossRef]
52. Menon, A.; Levermann, A.; Schewe, J.; Lehmann, J.; Frieler, K. Consistent increase in Indian monsoon rainfall and its variability across CMIP-5 models. *Earth Syst. Dyn.* **2013**, *4*, 287–300. [CrossRef]
53. Vinnarasi, R.C.T. Dhanya Changing characteristics of extreme wet and dry spells of Indian monsoon rainfall. *J. Geophys. Res. Atmos.* **2016**, *121*, 2146–2160. [CrossRef]
54. Vittal, H.; Ghosh, S.; Karmakar, S.; Pathak, A.; Murtugudde, R. Lack of dependence of Indian summer monsoon rainfall extremes on temperature: An observational evidence. *Sci. Rep.* **2016**, *6*, 31039. [CrossRef] [PubMed]
55. Devi, N.N.; Sridharan, B.; Kuiry, S.N. Impact of Urban Sprawl on Future Flooding in Chennai City, India Impact of Urban Sprawl on Future Flooding in Chennai City. *India. J. Hydrol.* **2019**, *574*, 486–496. [CrossRef]
56. Bollasina, M.A.; Ming, Y.; Ramaswamy, V. Anthropogenic aerosols and the weakening of the south Asian summer monsoon. *Science* **2011**, *334*, 502–505. [CrossRef]
57. Paul, S.; Ghosh, S.; Oglesby, R.; Pathak, A.; Chandrasekharan, A.; Ramsankaran, R. Weakening of Indian Summer Monsoon Rainfall due to Changes in Land Use Land Cover. *Sci. Rep.* **2016**, *6*, 32177. [CrossRef]
58. Ali, H.; Mishra, V. Contrasting response of rainfall extremes to increase in surface air and dewpoint temperatures at urban locations in India. *Sci. Rep.* **2017**, *7*, 1228. [CrossRef]
59. Dulal, K.N.; Takeuchi, K.; Ishidaira, H. Evaluation of the Influence of Uncertainty in Rainfall and Discharge Data on Hydrological Modeling. *Annu. J. Hydraul. Eng.* **2007**, *51*, 31–36. [CrossRef]
60. Daniel, J.A.; Staricka, J.A. Frozen soil impact on ground water–surface water interaction. *J. Am. Water Resour. Assoc.* **2000**, *36*, 151–160. [CrossRef]
61. Moss, R.H.; Edmonds, J.A.; Hibbard, K.A.; Manning, M.R.; Rose, S.K.; Van Vuuren, D.P.; Carter, T.R.; Emori, S.; Kainuma, M.; Kram, T.; et al. The next generation of scenarios for climate change research and assessment. *Nature* **2010**, *463*, 747–756. [CrossRef]
62. *IS 10500*; Indian Standard Drinking Water Specification (Second Revision). Bureau of Indian Standards (BIS): New Delhi, India, 2012.
63. Chinnasamy, P.; Agoramoorthy, G. Groundwater Storage and Depletion Trends in Tamil Nadu State, India. *Water Resour. Manag.* **2015**, *29*, 2139–2152. [CrossRef]
64. Senthilkumar, S.; Vinodh, K.; Babu, G.J.; Gowtham, B.; Arulprakasam, V. Integrated seawater intrusion study of coastal region of Thiruvallur district, Tamil Nadu, South India. *Appl. Water Sci.* **2019**, *9*, 124. [CrossRef]
65. Magistrali, I.C.; Delgado, R.C.; dos Santos, G.L.; Pereira, M.G.; de Oliveira, E.C.; Neves, L.D.O.; de Souza, L.P.; Teodoro, P.E.; Junior, C.A.S. Performance of CCCma and GFDL climate models using remote sensing and surface data for the state of Rio de Janeiro-Brazil. *Remote Sens. Appl. Soc. Environ.* **2021**, *21*, 100446. [CrossRef]
66. YoosefDoost, A.; Sadeghian, M.S.; Farahani, M.A.N.; Rasekhi, A. Comparison between performance of statistical and low cost ARIMA model with GFDL, CM2. 1 and CGM 3 atmosphere-ocean general circulation models in assessment of the effects of climate change on temperature and precipitation in Taleghan Basin. *Am. J. Water Resour.* **2017**, *5*, 92–99. [CrossRef]

67. Jury, M.R. Statistical evaluation of CMIP5 climate change model simulations for the Ethiopian highlands. *Int. J. Climatol.* **2015**, *35*, 37–44. [CrossRef]
68. Preetha, P.P.; Al-Hamdan, A.Z. Developing Nitrate-Nitrogen Transport Models using Remotely-Sensed Geospatial Data of Soil Moisture Profiles and Wet Depositions. *J. Environ. Sci. Health Part A* **2020**, *55*, 615–628. [CrossRef]
69. Preetha, P.P.; Al-Hamdan, A.Z. Integrating finite-element-model and remote-sensing data into SWAT to estimate transit times of nitrate in groundwater. *Hydrogeol. J.* **2020**, *28*, 1–19. [CrossRef]
70. Zeng, J.; Huang, G.; Mai, Y.; Chen, W. Optimizing the cost-effectiveness of low impact development (LID) practices using an analytical probabilistic approach. *Urban Water J.* **2017**, *2*, 136–143. [CrossRef]